Engineering Transactions, **73**(2): 199–218, 2025, https://doi.org/10.24423/engtrans.3427.2025
Institute of Fundamental Technological Research Polish Academy of Sciences (IPPT PAN)
Université de Lorraine • Poznan University of Technology

Research Paper

Impact of Spin Slip Conditions on the Axisymmetric Rotation of a Spherical Particle in a Couple Stress Fluid Within a Cavity

Shekhar NISHAD, Krishna Prasad MADASU*

Department of Mathematics, National Institute of Technology
Raipur, 492010, Chhattisgarh, India

*Corresponding Author e-mail: madaspra.maths@nitrr.ac.in, kpm973@gmail.com

This paper investigates the effect of spin slip condition on the flow of a couple stress fluid between two concentric spheres. The spherical particles rotate about the z-axis with different angular velocities Ω_1 and Ω_2 under the assumption of low Reynolds numbers. To solve the governing equations, we impose tangential slip and couple stress spin slip boundary conditions at the surfaces of the particle and the cavity wall. The nondimensional torque is computed, tabulated and graphically analyzed for various values of the separation parameter, couple stress viscosity, angular velocity ratio, tangential slip, and couple stress spin slip parameters. Our findings indicate that torque value increases with higher values of the couple stress viscosity parameter, separation parameter, tangential slip parameter, and spin slip parameter. However, the torque decreases as the angular velocity ratio increases. Furthermore, our results agree with previously published findings for cases with vanishing tangential slip and spin slip at the particle and cavity surfaces.

Keywords: couple stress fluid; spin slip effect; rotation; torque; spherical particle.

Copyright © 2025 The Author(s).
Published by IPPT PAN. This work is licensed under the Creative Commons Attribution License CC BY 4.0 (https://creativecommons.org/licenses/by/4.0/).

Nomenclature

A, B, C, D	–	arbitrary constants,
a, b	–	radius of spheres (inner and outer),
d_{ij}	–	deformation rate,
$\mathbf{e}_r$, $\mathbf{e}_\theta$, $\mathbf{e}_\varphi$	–	unit vectors along r, θ, φ directions,
$I_{1/2}(\cdot)$, $K_{1/2}(\cdot)$	–	modified Bessel functions of the first and second kind of order 1/2,
$I_{3/2}(\cdot)$, $K_{3/2}(\cdot)$	–	modified Bessel functions of the first and second kind of order 3/2,
$m_{r\theta}$	–	couple stress,
p	–	pressure of fluid,
$(r, \theta\varphi)$	–	spherical coordinate system,

T_c/T_0 – normalized torque,
$t_{r\varphi}$ – shear stress,
$\mathbf{v}$ – velocity vector.

Greek symbols

δ_{ij} – Kronecker delta,
ε_{ijk} – alternating tensor,
η, η' – couple stress viscosity coefficients,
μ – dynamic viscosity coefficient,
ξ_1, ξ_3 – tangential slip parameters,
ξ_2, ξ_4 – couple stress spin slip parameters,
Ω – angular velocity ratio,
$\boldsymbol{\omega}$ – vorticity vector,
Ω_1, Ω_2 – angular velocity of spheres (inner and outer).

1. Introduction

A non-Newtonian fluid differs from Newton's law of viscosity. One example of non-Newtonian fluid is the couple stress fluid, which illustrates the effects of couple stresses and body couples in a fluid medium. Examples of couple stress fluids include biological fluids, lubricants, liquid crystals, and fuels [1].

Numerous studies have explored fluid flow problems under no-slip conditions; however, this condition is not always applicable. As a result, many researchers have investigated conditions involving slip effects to analyze various fluid flow problems. Navier [2] introduced a slip boundary condition that establishes a proportional relationship between the tangential velocity of the fluid and the shear rate at the solid surface. Ellahi [3] studied fundamental flow problems involving Oldroyd eight-constant fluid. Ashmawy [4] examined micropolar fluid flow between parallel plates, considering both slip and spin slip conditions. Devakar *et al.* [5] investigated Couette-Poiseuille flow of couple stress fluids between parallel plates under velocity slip conditions. Recently, Nishad and Madasu [9] have explored the effect of the spin slip parameter on fundamental flow problems of couple stress fluids between two parallel plates.

Rotational motion and torque are interrelated concepts that are crucial in physics, engineering, and technology. They have broad applications and play an important role in understanding the rotational movement of objects. Rotational motion is essential in designing gears, turbines, engines, and other rotating machinery. It also helps explain natural spinning phenomena, such as spinning planets, turning wheels, and orbiting satellites. Chang and Keh [6] examined the creeping rotational motion of spheroidal particles under tangential slip conditions in a viscous fluid. Ashmawy [7] explored the slow, steady rotation of axisymmetric slip particle in an incompressible viscous fluid at low Reynolds numbers. Prasad *et al.* [8] provided exact solutions for axisymmetric

viscous fluid flow problems involving two concentric spheres rotating at different angular velocities while considering slip conditions at both the particle and container surfaces. Iyenger and Srinivasacharya [10] derived expressions for velocity and microrotation vectors in their study of an approximately spherical object's rotational motion in a micropolar fluid. El-Sapa *et al.* [11] investigated the quasi-steady motion of two spheres spinning along their common axis of symmetry in a viscous fluid.

Ashmawy [12] discussed the rotational movement of two spheres of arbitrary position in a couple stress fluids using the boundary collocation approach. In Newtonian fluids, Chou and Keh [13] investigated the rotational motion of spherical particle inside a spherical cavity with slip surfaces. Ashmawy [14] discussed the unsteady flow of a couple stress fluid past a rotating sphere. Al-Hanaya *et al.* [15] studied the steady motion of a couple stress fluid between two non-concentric rotating spherical surfaces with different angular velocities around a common diameter. El-Sapa and Almoneef [16] used spin slip and slip conditions to study the translational motion of a solid sphere in a couple stress fluid. El-Sapa and Al-Hanaya [17] discussed the influence of permeability and slippage on the torque of rotating concentric spheres filled with Brinkman couple stress fluid. Al-Hanaya and El-Sapa [18] analyzed the rotational motion of a couple stress fluid between two concentric spheres under the effects of a magnetic field and slippage. Sarkar and Madasu [19] investigated the effect of the tangential slip parameter on couple stress fluid flow past a cylindrical particle embedded in a porous medium. Recently, Alotaibi and El-Sapa [20] studied magnetohydrodynamic (MHD) couple stress fluid flow between two concentric spheres, calculating and analyzing the drag force on the inner sphere under tangential slip [19, 20] and couple stress spin conditions [20]. To the best of our knowledge, no published results exist on the rotational motion of a couple stress fluid between two concentric spheres with tangential and couple stress spin slip boundary conditions.

In this research, we investigate the flow of a couple stress fluid that moves steadily and slowly between two concentric spherical boundaries. The spherical surfaces rotate about the z-axis at different angular velocities under velocity slip and spin slip conditions. This study extends the work of Al-Hanaya *et al.* [15] to the concentric case, incorporating tangential and couple stress slip at the boundaries of both the inner and outer spheres.

2. Mathematical model

Consider the rotational motion of a spherical solid particle in a concentric spherical cavity. The fluid flow is assumed to be steady, incompressible, and axisymmetric. Assume the inner and outer spheres have radii a and b, respectively,

with the gap is filled with a couple stress fluid. The inner and outer spheres rotate about the z-axis with different angular velocities Ω_1 and Ω_2, respectively.

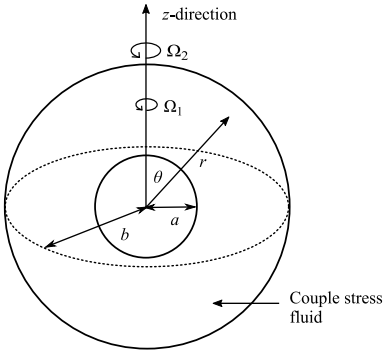

FIG. 1. Physical representation of the problem.

The governing equations of couple stress fluid flow with zero body couple and body force are given as [1]:

$$\nabla \cdot \mathbf{v} = 0, \tag{2.1}$$

$$\nabla p + \mu \nabla^2 \mathbf{v} + \eta \nabla^4 \mathbf{v} = 0, \tag{2.2}$$

where $\mathbf{v}$, p, μ, and η denote the fluid velocity, fluid pressure, viscosity coefficient of a classical fluid, and the first viscosity coefficient of a couple stress fluid, respectively. When $\eta = 0$, Eq. (2.2) reduces to the Stokes equation.

The constitutive relationships for a couple stress fluid are given by [1]:

$$t_{ij} = -p\delta_{ij} + 2\mu d_{ij} - \frac{1}{2}\varepsilon_{ijk} m_{sk,s}, \tag{2.3}$$

$$m_{ij} = m\delta_{ij} + 4\eta' \omega_{j,i} + 4\eta \omega_{i,j}, \tag{2.4}$$

where m, δ_{ij}, d_{ij}, ε_{ijk} represent the trace of the couple stress tensor, Kronecker delta, deformation rate tensor, and alternating tensor, respectively. The parameter η denotes the second viscosity coefficient of the couple stress fluid. The viscosity coefficients satisfy the following inequalities:

$$\mu \geq 0; \qquad \eta \geq 0; \qquad \eta \geq \eta' \geq -\eta.$$

The vorticity vector is defined as [1]:

$$\boldsymbol{\omega} = \frac{1}{2} \times \mathbf{v}. \tag{2.5}$$

The Kronecker delta, deformation rate tensor, and alternating tensor are defined as [1]:

$$\delta_{ij} = \begin{cases} 1, & \text{for } i = j, \\ 0, & \text{for } i \neq j, \end{cases}$$

$$d_{ij} = \frac{1}{2}(v_{i,j} + v_{j,i}),$$

$$\varepsilon_{ijk} = \begin{cases} 1, & \text{for } \varepsilon_{123}, \varepsilon_{231}, \varepsilon_{312}, \\ -1, & \text{for } \varepsilon_{132}, \varepsilon_{321}, \varepsilon_{213}, \\ 0, & \text{otherwise.} \end{cases}$$

Let (r, θ, φ) be the spherical coordinate system with the origin O as the center of the particle. Hence, the velocity and vorticity vectors are given as:

$$\mathbf{v} = v_\varphi(r,\theta)\mathbf{e}_\varphi, \qquad \boldsymbol{\omega} = \omega_r(r,\theta)\mathbf{e}_r + \omega_\theta(r,\theta)\mathbf{e}_\theta, \tag{2.6}$$

where $\mathbf{e}_r$, $\mathbf{e}_\theta$ and $\mathbf{e}_\varphi$ are unit vectors along r, θ, and φ-directions, respectively.

2.1. Boundary conditions

In order to obtain the solution to the problem, we apply the appropriate boundary conditions, which are significant both physically and mathematically. For the present problem, we consider two types of boundary conditions: (i) tangential slip boundary conditions [2, 8, 9], which ensure a proportional relationship between shear stress and velocity, and (ii) mixed-type boundary conditions [1, 9, 15], which define the relationship between vorticity components and couple stress. In this study, we apply these boundary conditions, which are practical and realistic for slip surfaces:

$$\lambda_1(v_\varphi - r\,\Omega_1 \sin\theta) = t_{r\varphi}, \qquad m_{r\theta} = \lambda_2\omega_\theta \quad \text{at } r = a, \tag{2.7}$$

$$-\lambda_3(v_\varphi - r\,\Omega_2 \sin\theta) = t_{r\varphi}, \qquad m_{r\theta} = -\lambda_4\omega_\theta \text{ at } r = b. \tag{2.8}$$

where λ_i are the tangential slip parameters, and λ_j are the spin slip parameters at particle and cavity wall surfaces, respectively, where $i = 1, 3$ and $j = 2, 4$.

Introducing non-dimensional variables: $r = a\widetilde{r}$, $v_\varphi = \Omega_1 a\,\widetilde{v}_\varphi$, $\nabla = \widetilde{\nabla}/a$ in Eq. (2.2) and the boundary conditions, Eqs. (2.7) and (2.8), and dropping the tildes, we obtain:

$$E^2(E^2 - l^2)\,(r\sin\theta\, v_\varphi) = 0, \tag{2.9}$$

$$\xi_1(v_\varphi - r\sin\theta) = t_{r\varphi}, \qquad m_{r\theta} = \xi_2\omega_\theta \quad \text{at } r = 1, \tag{2.10}$$

$$-\xi_3(v_\varphi - r\,\Omega\sin\theta) = t_{r\varphi}, \qquad m_{r\theta} = -\xi_4\omega_\theta \text{ at } r = 1/\lambda, \tag{2.11}$$

where

$$E^2 = \frac{\partial^2}{\partial r^2} - \frac{\cot\theta}{r^2}\frac{\partial}{\partial\theta} + \frac{1}{r^2}\frac{\partial^2}{\partial\theta^2}$$

is the Stokesian operator, and

$$l^2 = \frac{a^2\mu}{\eta}, \qquad \xi_1 = \frac{\lambda_1 a}{\mu}, \qquad \xi_2 = \frac{\lambda_2}{\mu a}, \qquad \xi_3 = \frac{\lambda_3 a}{\mu}, \qquad \xi_4 = \frac{\lambda_4}{\mu a},$$
$$\Omega = \frac{\Omega_2}{\Omega_1}, \qquad \lambda = \frac{a}{b}.$$

The solution to Eq. (2.9) is given by:

$$v_\varphi(r,\theta) = \Big(Ar^{-2} + Br + Cr^{-1/2}I_{3/2}(lr) + Dr^{-1/2}K_{3/2}(lr)\Big)\sin\theta, \tag{2.12}$$

where A, B, C, D are arbitrary constants, and $I_{3/2}(lr)$ and $K_{3/2}(lr)$ denote the modified Bessel functions of the first and second kind of order 3/2, respectively. Note that the detail solution of Eq. (2.9) is provided in the Appendix section.

The vorticity components, couple stress and shear rate are given by:

$$\omega_r = \Big(Ar^{-3} + B + Cr^{-3/2}I_{3/2}(lr) + Dr^{-3/2}K_{3/2}(lr)\Big)\cos\theta, \tag{2.13}$$

$$\omega_\theta = \frac{1}{2}\Big[Ar^{-3} - 2B + Cr^{-3/2}\Big(I_{3/2}(lr) - lrI_{1/2}(lr)\Big) + Dr^{-3/2}\Big(K_{3/2}(lr) + lrK_{1/2}(lr)\Big)\Big]\sin\theta, \tag{2.14}$$

$$m_{r\theta} = -2\Big[3(\eta+\eta')Ar^{-4} + Cr^{-5/2}\Big(\big(l^2r^2\eta + 3(\eta+\eta')\big)I_{3/2}(lr) - lr(\eta+\eta')I_{1/2}(lr)\Big) + Dr^{-5/2}\Big(\big(l^2r^2\eta + 3(\eta+\eta')\big)K_{3/2}(lr) + lr(\eta+\eta')K_{1/2}(lr)\Big)\Big]\sin\theta, \tag{2.15}$$

$$t_{r\varphi} = -\frac{1}{2}\Big\{A\Big[6\mu r^{-3} + 12(\eta+\eta')r^{-5}\Big] + C\Big[I_{3/2}(lr)\big(6\mu r^2 + 12(\eta+\eta') - 2l^2r^2\eta\big) - lrI_{1/2}(lr)\big(2\mu r^2 - 2l^2r^2\eta + 4(\eta+\eta')\big)\Big]r^{-7/2} + D\Big[K_{3/2}(lr)\big(6\mu r^2 + 12(\eta+\eta') - 2l^2r^2\eta\big) + lrK_{1/2}(lr)\big(2\mu r^2 - 2l^2r^2\eta + 4(\eta+\eta')\big)\Big]r^{-7/2}\Big\}\sin\theta. \tag{2.16}$$

Using Eqs. (2.12)–(2.16), the boundary conditions (2.10) and (2.11) reduce to:

$$
\begin{aligned}
(2.17)\qquad & A\Big[\xi_1+3a^{-2}+6(\chi_1+\chi_2)\Big]+\xi_1 B \\
&\quad + C\Big\{I_{3/2}(l)\Big[\xi_1+3a^{-2}+6(\chi_1+\chi_2)-1\Big] \\
&\quad - lI_{1/2}(l)\Big[a^{-2}+2(\chi_1+\chi_2)-1\Big]\Big\} \\
&\quad + D\Big\{K_{3/2}(l)\Big[\xi_1+3a^{-2}+6(\chi_1+\chi_2)-1\Big] \\
&\quad + lK_{1/2}(l)\Big[a^{-2}+2(\chi_1+\chi_2)-1\Big]\Big\}-\xi_1=0,
\end{aligned}
$$

$$
\begin{aligned}
(2.18)\qquad & A\Big[3a^{-2}\lambda^3+6(\chi_1+\chi_2)\lambda^5-\xi_3\lambda^2\Big]-\xi_3 B\lambda^{-1} \\
&\quad + C\lambda^{7/2}\{I_{3/2}(l\lambda^{-1})\Big[3a^{-2}\lambda^{-2}+6(\chi_1+\chi_2)-\lambda^{-2}-\xi_3\lambda^{-3}\Big] \\
&\quad - l\lambda^{-1}I_{1/2}(l\lambda^{-1})\Big[a^{-2}\lambda^{-2}-\lambda^{-2}+2(\chi_1+\chi_2)\Big]\Big\} \\
&\quad + D\lambda^{7/2}\Big\{K_{3/2}(l\lambda^{-1})\Big[3a^{-2}\lambda^{-2}+6(\chi_1+\chi_2)-\lambda^{-2}-\xi_3\lambda^{-3}\Big] \\
&\quad + l\lambda^{-1}K_{1/2}(l\lambda^{-1})\Big[a^{-2}\lambda^{-2}-\lambda^{-2}+2(\chi_1+\chi_2)\Big]\Big\}+\xi_3\Omega\lambda^{-1}=0,
\end{aligned}
$$

$$
\begin{aligned}
(2.19)\qquad & A\Big[\xi_2+12(\chi_1+\chi_2)\Big]-2B\xi_2 \\
&\quad + C\Big\{I_{3/2}(l)\Big[\xi_2+4+12(\chi_1+\chi_2)\Big]-I_{1/2}(l)l\Big[\xi_2+4(\chi_1+\chi_2)\Big]\Big\} \\
&\quad + D\Big\{K_{3/2}(l)\Big[\xi_2+4+12(\chi_1+\chi_2)\Big]+K_{1/2}(l)l\Big[\xi_2+4(\chi_1+\chi_2)\Big]\Big\}=0,
\end{aligned}
$$

$$
\begin{aligned}
(2.20)\qquad & A\Big[12(\chi_1+\chi_2)\lambda^4-\xi_4\lambda^3\Big]+2B\xi_4 \\
&\quad + C\lambda^{5/2}\Big\{I_{3/2}(l\lambda^{-1})\Big[4\lambda^{-2}+12(\chi_1+\chi_2)-\xi_4\lambda^{-1}\Big] \\
&\quad - I_{1/2}(l\lambda^{-1})l\Big[4(\chi_1+\chi_2)\lambda^{-1}-\xi_4\lambda^{-2}\Big]\Big\} \\
&\quad + D\lambda^{5/2}\Big\{K_{3/2}(l\lambda^{-1})\Big[4\lambda^{-2}+12(\chi_1+\chi_2)-\xi_4\lambda^{-1}\Big] \\
&\quad + K_{1/2}(l\lambda^{-1})l\Big[4(\chi_1+\chi_2)\lambda^{-1}-\xi_4\lambda^{-2}\Big]\Big\}=0,
\end{aligned}
$$

where $\chi_1=\frac{\eta}{\mu a^2}$, $\chi_2=\frac{\eta'}{\mu a^2}$, $l=\frac{1}{\sqrt{\chi_1}}$. Expressions for A, B, C, and D are long, and, therefore, we have not included them in the paper.

The corresponding torque on the axisymmetric object is calculated as follows [14]:

$$T_c = 2\pi\,\mu a^3 \int_0^{\pi} t_{r\varphi}|_{r=1}\,\mathrm{d}\theta. \tag{2.21}$$

The resultant torque is given as:

$$\begin{aligned} T_c = -\frac{4}{3}\pi\,\mu a^3 \Big\{ & A\Big[6 + 12(\chi_1+\chi_2)\Big] \\ & + C\Big[I_{3/2}(l)\,(4 + 12(\chi_1+\chi_2)) - 4lI_{1/2}(l)(\chi_1+\chi_2)\Big] \\ & + D\Big[K_{3/2}(l)\,(4 + 12(\chi_1+\chi_2)) + 4lK_{1/2}(l)(\chi_1+\chi_2)\Big]\Big\}. \end{aligned} \tag{2.22}$$

When a spherical particle with radius a rotates in an incompressible viscous fluid in an unbounded region with an angular velocity Ω_1, the torque experienced is:

$$T_0 = -8\pi\,\mu a^3 \Omega_1. \tag{2.23}$$

3. Results and discussion

In this work, we have obtained the normalized torque $T(= T_c/T_0)$ exerted by a couple stress fluid on the rotational motion of two spherical particles, using tangential and spin slip boundary conditions at the particle and cavity surfaces. We present numerical results in Tables 1–5 and graphical results in Figs. 2–12. The normalized torque T versus the separation parameter λ for different values of the ratio of angular velocities Ω, the couple stress viscosity parameters χ_1 and χ_2, velocity slip parameters ξ_1 and ξ_3, and spin slip parameters ξ_2 and ξ_4 are shown.

Tables 1–5 display the values of the normalized torque acting on the inner sphere for various values of the parameters λ, Ω, ξ_1, ξ_2, ξ_3, ξ_4, χ_1, and $\chi_2 = 0$. The findings show that the torque increases monotonically with an increase in the radius ratio. The fact that a rise in χ_1 also results in an increase in the torque value is significant. When $\tau = -1$, i.e., $\eta' = -\eta$, the normalized torque exerted by a consistent couple stress fluid [21] on the inner sphere is shown in Tables 4 and 5. Table 4 shows that as the separation parameter λ and tangential slip parameters δ increase, T also increases. Table 5 presents the fact that T declines with a decrease in the separation parameter λ and increases with an increase in the angular velocity ratio Ω. If the couple stress coefficient χ_1 is assumed to be very small, our results are in good agreement with the case of vanishing tangential slip and couple stress spin slip at the boundaries of the particle and cavity.

TABLE 1. The normalized torque on the inner sphere for different values of $\xi_1 = \xi_3 = \delta$ and λ with $\Omega = 0$, $\chi_1 = 0.01$, $\chi_2 = 0.0$, $\xi_2 = \xi_4 = \gamma \to 0$.

λ	T			
	$\delta = 5$	$\delta = 7$	$\delta = 20$	$\delta \to \infty$
0.1	0.63601	0.71385	0.89106	1.02824
0.3	0.64467	0.72550	0.91114	1.05640
0.5	0.67262	0.76653	0.99148	1.17711
0.7	0.72484	0.85688	1.21719	1.57252
0.8	0.75924	0.92983	1.46460	2.11970
0.9	0.79682	1.02978	1.96179	3.81943
0.99	0.82992	1.15099	3.09935	34.31210
0.999	0.83300	1.16509	3.30828	288.442

TABLE 2. The normalized torque on inner sphere for different values of γ and λ with $\chi_1 = 0.01$, $\chi_2 = 0.0$, $\Omega = 0$, $\delta \to \infty$.

λ	T			
	$\gamma = 0$ (vanishing couple stress)	$\gamma = 0.1$	$\gamma = 0.2$	$\gamma \to \infty$
0.1	1.02855	1.03247	1.03523	1.05127
0.3	1.05673	1.06207	1.06584	1.08794
0.5	1.17755	1.19281	1.20385	1.27278
0.7	1.57343	1.65318	1.71551	2.22713
0.8	2.12156	2.36582	2.57095	4.94521
0.9	3.82648	5.12022	6.30573	33.5891
0.99	34.9953	197.439	358.214	31448.0
0.999	346.281	15404.7	27953.1	$1.6595 \cdot 10^5$

TABLE 3. The normalized torque for various values of χ_1 and λ when tangential slip and couple stress spin slip vanishes at the particle and cavity surfaces, i.e., $\delta \to \infty$ and $\gamma \to 0$, and $\Omega = 0$.

λ	T			
	$\chi_1 = 0.001$	$\chi_1 = 0.01$	$\chi_1 = 0.1$	$\chi_1 = 0.5$
0.1	1.00392	1.02855	1.24342	2.06483
0.3	1.03081	1.05673	1.28367	2.16675
0.5	1.14653	1.17755	1.45006	2.56781
0.7	1.52762	1.57344	1.98572	3.78302
0.8	2.05718	2.12158	2.72680	5.40453
0.9	3.70500	3.82662	5.02800	10.3659
0.99	33.8121	35.0117	47.0060	100.294
0.999	335.986	347.937	467.352	996.021

TABLE 4. Torque exerted by the consistent couple stress fluid ($\tau = -1$) for various values of λ and δ with $\Omega = -1$.

δ	T			
	$\lambda = 0.1$	$\lambda = 0.3$	$\lambda = 0.6$	$\lambda = 0.9$
0.01	0.00664	0.00658	0.00587	0.00401
0.1	0.06451	0.06406	0.05767	0.04002
1	0.50009	0.50034	0.47929	0.38172
3	1.00047	1.00956	1.04518	1.03786
5	1.25075	1.26757	1.36826	1.58155
10	1.53964	1.56814	1.78121	2.60507
20	1.74065	1.77906	2.09778	3.85185
10^5	2.00144	2.05491	2.55070	7.36959

TABLE 5. Torque exerted by the consistent couple stress fluid ($\tau = -1$) for various values of Ω and λ with $\delta \to \infty$, $\gamma = 0.001$.

Ω	T			
	$\lambda = 0.1$	$\lambda = 0.3$	$\lambda = 0.6$	$\lambda = 0.9$
-3	4.00379	4.11114	5.10364	14.7966
-2	3.00279	3.08327	3.82756	11.0967
-1	2.00179	2.05540	2.55148	7.39674
0	1.00078	1.02753	1.27539	3.69679
0.1	0.90068	0.92474	1.14779	3.32679
0.3	0.70048	0.71917	0.89257	2.58680
0.5	0.50028	0.51360	0.63735	1.84681
1	$-2.1713 \cdot 10^{-4}$	$-3.3457 \cdot 10^{-4}$	$-6.8669 \cdot 10^{-4}$	$-0.0031 \cdot 10^{-4}$

3.1. Special cases

Case I: For the case where the tangential slip and couple stress spin slip parameters vanish at the particle and cavity surfaces:

The behavior of normalized torque, as shown in Table 3, matches the results of AL-HANAYA *et al.* [15].

Case II: We have obtained the consistent couple stress fluid case, where the ratio of the first and second couple stress viscosity coefficients is -1, i.e., $\tau = -1$, by solving the following system of linear Eqs. (3.1)–(3.4):

$$
\begin{aligned}
(3.1)\quad & A\left[\xi_1 + 3a^{-2} + 6(1+\tau)\right] + \xi_1 B \\
& + C\Big\{ I_{3/2}(l)\Big[\xi_1 + 3a^{-2} + 6(1+\tau) - 1\Big] - lI_{1/2}(l)\Big[a^{-2} + 2(1+\tau) - 1\Big]\Big\} \\
& + D\Big\{ K_{3/2}(l)\Big[\xi_1 + 3a^{-2} + 6(1+\tau) - 1\Big] \\
& + lK_{1/2}(l)\Big[a^{-2} + 2(1+\tau) - 1\Big]\Big\} - \xi_1 = 0,
\end{aligned}
$$

$$
\begin{aligned}
(3.2)\quad & A\left[3a^{-2}\lambda^3+6(1+\tau)\lambda^5-\xi_3\lambda^2\right]-\xi_3 B\lambda^{-1}\\
&+C\lambda^{7/2}\Big\{I_{3/2}(l\lambda^{-1})\Big[3a^{-2}\lambda^{-2}+6(1+\tau)-\lambda^{-2}-\xi_3\lambda^{-3}\Big]\\
&\quad-l\lambda^{-1}I_{1/2}(l\lambda^{-1})\Big[a^{-2}\lambda^{-2}-\lambda^{-2}+2(1+\tau)\Big]\Big\}\\
&+D\lambda^{7/2}\Big\{K_{3/2}(l\lambda^{-1})\Big[3a^{-2}\lambda^{-2}+6(1+\tau)-\lambda^{-2}-\xi_3\lambda^{-3}\Big]\\
&+l\lambda^{-1}K_{1/2}(l\lambda^{-1})\Big[a^{-2}\lambda^{-2}-\lambda^{-2}+2(1+\tau)\Big]\Big\}+\xi_3\Omega\lambda^{-1}=0,\\
(3.3)\quad & A\left[\xi_2+12(1+\tau)\right]-2B\xi_2\\
&+C\Big\{I_{3/2}(l)\Big[\xi_2+4+12(1+\tau)\Big]-I_{1/2}(l)l\Big[\xi_2+4(1+\tau)\Big]\Big\}\\
&+D\Big\{K_{3/2}(l)\Big[\xi_2+4+12(1+\tau)\Big]+K_{1/2}(l)l\Big[\xi_2+4(1+\tau)\Big]\Big\}=0,\\
(3.4)\quad & A\left[12(1+\tau)\lambda^4-\xi_4\lambda^3\right]+2B\xi_4\\
&+C\lambda^{5/2}\Big\{I_{3/2}(l\lambda^{-1})\Big[4\lambda^{-2}+12(1+\tau)-\xi_4\lambda^{-1}\Big]\\
&\quad-I_{1/2}(l\lambda^{-1})l\Big[4(1+\tau)\lambda^{-1}-\xi_4\lambda^{-2}\Big]\Big\}\\
&+D\lambda^{5/2}\Big\{K_{3/2}(l\lambda^{-1})\Big[4\lambda^{-2}+12(1+\tau)-\xi_4\lambda^{-1}\Big]\\
&+K_{1/2}(l\lambda^{-1})l\Big[4(1+\tau)\lambda^{-1}-\xi_4\lambda^{-2}\Big]\Big\}=0.
\end{aligned}
$$

Figures 2 and 3 show the variation of normalized torque versus the separation parameter λ for different values of first and second couple stress viscosity (χ_1, χ_2). It is observed that the normalized torque increases gradually as the separation parameter increases. It is also observed that the effect is more pronounced for higher couple stress viscosity parameter.

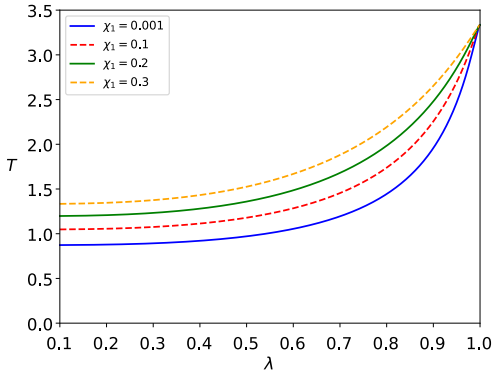

FIG. 2. Variation of torque versus λ with $\chi_2 = 0$, $\Omega = 0$, $\delta = 7$, $\gamma = 0.01$.

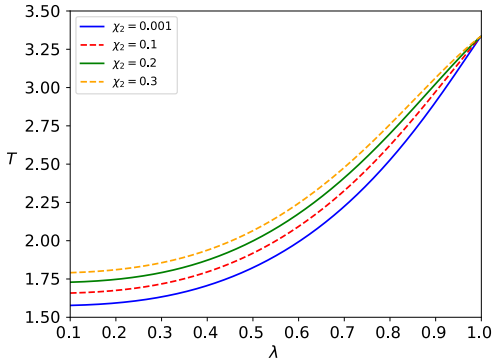

FIG. 3. Variation of torque versus λ with $\chi_1 = 0.5$, $\Omega = 0$, $\delta = 20$, and $\gamma = 0.01$.

In Fig. 4, it is observed that as the boundaries of both spheres come closer to each other, the torque also increases. This effect is most significant for a low angular velocity ratio. Figure 5 shows that the normalized torque is an increasing function of both the separation parameter λ and the couple stress viscosity parameter χ_1.

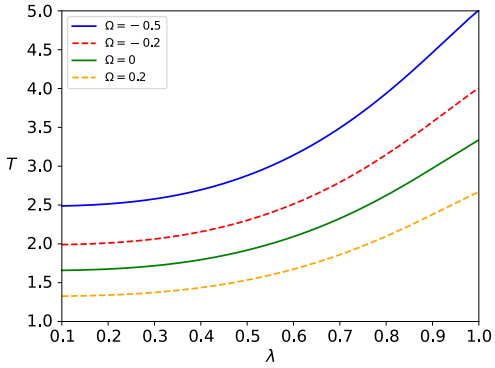

FIG. 4. Variation of torque versus λ with $\chi_2 = 0.1$, $\chi_1 = 0.5$, $\delta = 20$, and $\gamma = 0.1$.

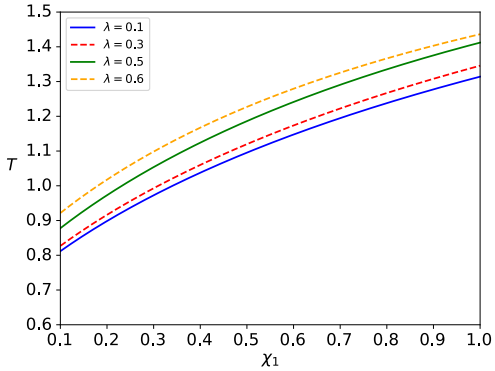

FIG. 5. Variation of torque versus χ_1 with $\chi_2 = 0$, $\Omega = 0$, $\delta = 7$, and $\gamma = 0.1$.

Figures 6–8 depict the variation of torque versus the separation parameter λ for different values of tangential slip parameters. it is observed that the normalized torque increases with an increase in the value of the tangential slip parameter. It is observed that normalized torque increases as the tangential

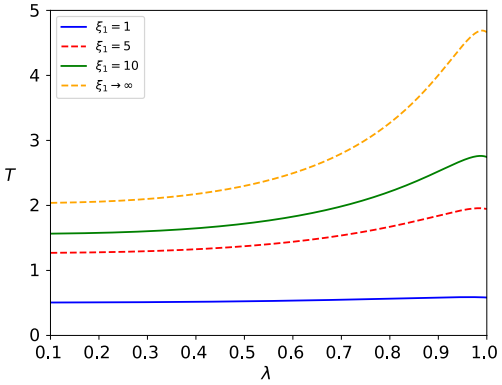

FIG. 6. Variation of torque versus λ with $\tau = -1$, $\xi_3 = 7$, $\chi_1 = 0.1$, $\Omega = -1$, and $\delta = 0.1$.

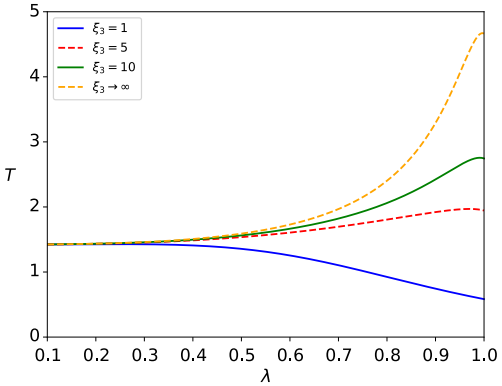

FIG. 7. Variation of torque versus λ with $\tau = -1$, $\xi_1 = 7$, $\Omega = -1$, and $\gamma = 0.1$.

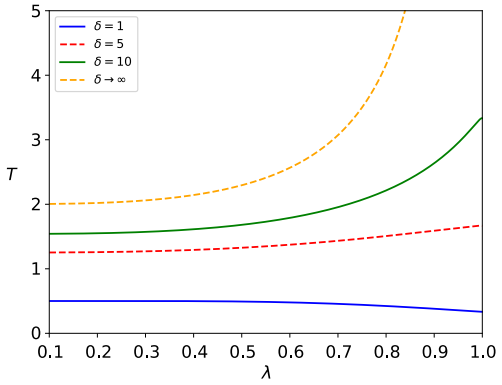

FIG. 8. Variation of torque versus λ with $\chi_2 = 0.001$, $\tau = -1$, $\Omega = -1$, and $\gamma = 0.1$.

slip parameter rises, and the variation normalized torque is more significant when the slip parameter is high.

In Figs. 9–11, it is observed that the value of the normalized torque increases as the separation parameter rises. Furthermore, the torque shows high variation

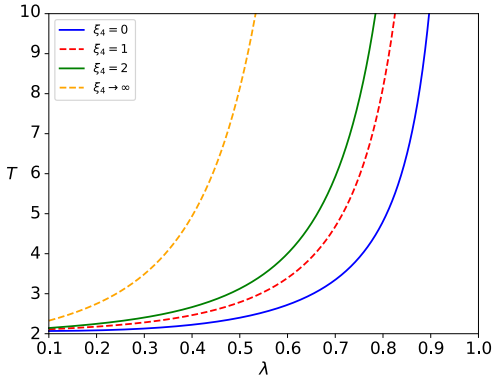

FIG. 9. Variation of torque versus λ with $\tau = -1$, $\xi_2 = 0.2$, $\delta \to \infty$, and $\Omega = -1$.

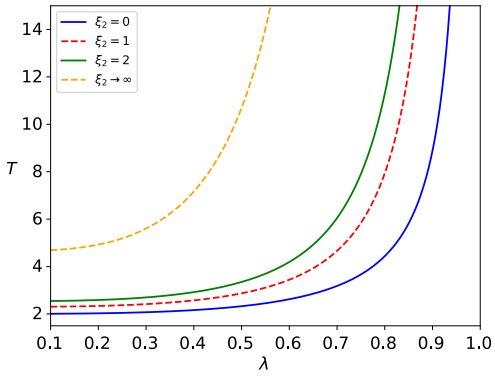

FIG. 10. Variation of torque versus λ with $\tau = -1$, $\xi_4 = 0.2$, $\delta \to \infty$, and $\Omega = -1$.

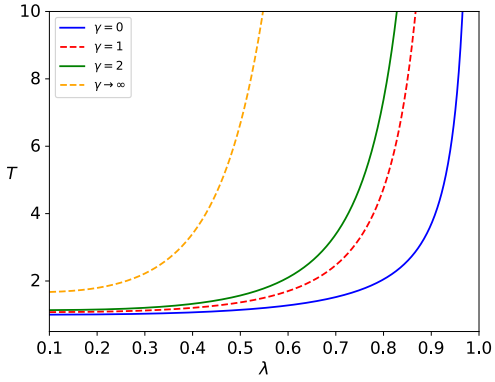

FIG. 11. Variation of torque versus λ with $\tau = -1$, $\delta \to \infty$, and $\Omega = -1$.

for higher values of spin slip parameter, similar to the behavior observed in the case of tangential slip parameter. Figure 12 shows that the normalized torque increases with the separation parameter λ, and is higher when the inner and outer spheres rotate in opposite directions (i.e., more negative Ω).

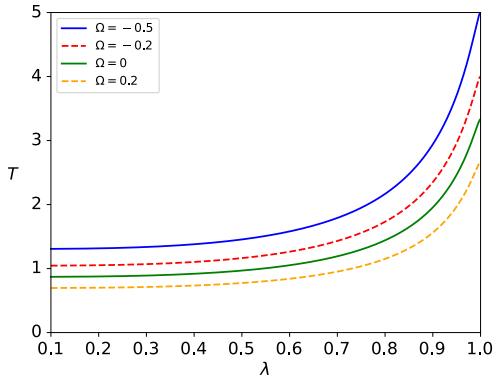

FIG. 12. Variation of torque versus λ with $\tau = -1$, $\delta = 20$ and $\gamma = 0.1$.

Similar trends for the properties of couple stress viscosity properties are observed in the study of AL-HANAYA *et al.* [15].

4. CONCLUSIONS

The axisymmetric steady rotational motion of a couple stress fluid between concentric spheres with slip boundary conditions has been examined. An analytical expression for the torque on the inner sphere has been derived. Based on the data presented in the tables and graphs, the following observations can be made from this study:

1) The effect of the couple stress viscosity parameters increases the normalized torque acting on the inner sphere.
2) Both tangential slip and couple stress spin slip parameters lead to an increase in the torque value.
3) It is found that the higher values of the angular velocity ratio Ω lead to a decline in the normalized torque.

The limiting cases where $\delta \to \infty$ and $\gamma \to 0$ have been derived for the present problem. Notably, the limiting solutions show significant agreement with the previous results of AL-HANAYA *et al.* [15] for no slip and no spin slip boundary conditions. Future work could consider various problems, such as non-Newtonian fluid flow between two approximate spheres and cylinder with slippage and spin conditions.

Appendix. Solution for the differential equation

The fourth order linear homogeneous partial differential equation is:

$$E^2(E^2 - l^2)(r \sin\theta\, v_\varphi) = 0, \tag{A.1}$$

where

$$E^2 = \frac{\partial^2}{\partial r^2} - \frac{\cot\theta}{r^2}\frac{\partial}{\partial\theta} + \frac{1}{r^2}\frac{\partial^2}{\partial\theta^2}$$

is the Stokesian operator.

$$E^2(E^2 - l^2)W = 0, \quad \text{where} \quad W = r\sin\theta\, v_\varphi. \tag{A.2}$$

Let the solutions of $E^2W = 0$, $(E^2 - l^2)W = 0$ be W_1 and W_2, respectively. Thus, $W = W_1 + W_2$ is the solution of corresponding homogeneous equation $E^2(E^2 - l^2)W = 0$. Now, we discuss the solution of $E^2W_1 = 0$ as follows:

$$\frac{\partial^2 W_1}{\partial r^2} - \frac{\cot\theta}{r^2}\frac{\partial W_1}{\partial\theta} + \frac{1}{r^2}\frac{\partial^2 W_1}{\partial\theta^2} = 0. \tag{A.3}$$

Assume the solution is of the form $W_1 = F(r)\sin^2\theta$. Then Eq. (A.3) reduces to:

$$\left(\frac{\partial^2}{\partial r^2} - \frac{2}{r^2}\right) F(r)\sin^2\theta = 0, \tag{A.4}$$

$$\Longrightarrow r^2F''(r) - 2F(r) = 0, \tag{A.5}$$

which is a second-order Cauchy–Euler differential equation, whose general solution is [22]:

$$F(r) = \frac{A}{r} + Br^2,$$

$$\Rightarrow W_1 = \left(\frac{A}{r} + Br^2\right)\sin^2\theta.$$

Here, we discuss the solution of $(E^2 - l^2)W_2 = 0$ as follows:

$$\frac{\partial^2 W_2}{\partial r^2} - \frac{\cot\theta}{r^2}\frac{\partial W_2}{\partial\theta} + \frac{1}{r^2}\frac{\partial^2 W_2}{\partial\theta^2} - l^2W_2 = 0. \tag{A.6}$$

Assume the solution is of the form $W_2 = F(r)\sin^2\theta$. Then, Eq. (A.6) reduces to:

$$r^2\frac{\mathrm{d}^2F}{\mathrm{d}r^2} - (l^2r^2 + 2)F = 0. \tag{A.7}$$

Let $lr = t \Rightarrow r = \frac{t}{l}$. Then:

$$F'(r) = l\frac{\mathrm{d}F}{\mathrm{d}t},$$

$$F''(r) = l^2\frac{\mathrm{d}^2F}{\mathrm{d}t^2}.$$

Substituting $F'(r)$ and $F''(r)$ into Eq. (A.7), we get:

$$t^2\frac{\mathrm{d}^2F}{\mathrm{d}t^2} - (t^2+2)F = 0. \tag{A.8}$$

Let $F = \sqrt{t}Z$. Then:

$$\frac{\mathrm{d}F}{\mathrm{d}t} = \frac{1}{2}t^{-1/2}Z + t^{1/2}\frac{\mathrm{d}Z}{\mathrm{d}t},$$

$$\frac{\mathrm{d}^2F}{\mathrm{d}t^2} = -\frac{1}{4}t^{-3/2}Z + t^{-1/2}\frac{\mathrm{d}Z}{\mathrm{d}t} + t^{1/2}\frac{\mathrm{d}^2Z}{\mathrm{d}t^2}.$$

Substituting F and $\frac{\mathrm{d}^2F}{\mathrm{d}t^2}$ into Eq. (A.8), we get:

$$t^{5/2}\frac{\mathrm{d}^2Z}{\mathrm{d}t^2} + t^{3/2}\frac{\mathrm{d}Z}{\mathrm{d}t} - \left(t^{5/2} + \frac{9}{4}t^{1/2}\right)Z = 0.$$

Dividing both sides by $t^{1/2}$:

$$\Rightarrow t^2\frac{\mathrm{d}^2Z}{\mathrm{d}t^2} + t\frac{\mathrm{d}Z}{\mathrm{d}t} - \left(t^2 + \frac{9}{4}\right)Z = 0. \tag{A.9}$$

Equation (A.9) represents the modified Bessel's equation, so the solution is of the form [10, 23–26]:

$$Z = C^*I_{3/2}(t) + D^*K_{3/2}(t),$$

$$F = C^*\sqrt{t}I_{3/2}(t) + D^*\sqrt{t}K_{3/2}(t).$$

Therefore,

$$F(r) = C\sqrt{r}I_{3/2}(lr) + D\sqrt{r}K_{3/2}(lr),$$

where $C = C^*\sqrt{l}$, $D = D^*\sqrt{l}$. Thus, $W_2 = \left(C\sqrt{r}I_{3/2}(lr) + D\sqrt{r}K_{3/2}(lr)\right)\sin^2\theta$, and by the principle of superposition,

$$W = W_1 + W_2 = \left(\frac{A}{r} + Br^2 + C\sqrt{r}I_{3/2}(lr) + D\sqrt{r}K_{3/2}(lr)\right)\sin^2\theta$$

is the solution of Eq. (A.2).

$$\Rightarrow v_\varphi(r,\theta) = \left(\mathrm{A}r^{-2} + Br + Cr^{-1/2}I_{3/2}(lr) + Dr^{-1/2}K_{3/2}(lr)\right)\sin\theta$$

is the solution of the Eq. (A.1).

Acknowledgments

The first author, S. Nishad, is deeply thankful for the institute research fellowship from the National Institute of Technology, Raipur.

Conflict of interest

The authors have no conflicts to disclose.

References

1. Stokes V.K., *Theories of Fluids with Microstructure: An Introduction*, Springer Science & Business Media, 2012.

2. Navier C.L.M.H., Note on the laws of fluid motion [in French: Mémoire sur les lois du Mouvement des Fluides], *Mémoires de l'Académie Royale des Sciences de l'Institut de France*, **6**: 389–440, 1823.

3. Ellahi R., Effects of the slip boundary conditions on non-Newtonian flows in a channel, *Communications in Nonlinear Science and Numerical Simulation*, **14**(4): 1377–1384, 2009, https://doi.org/10.1016/j.cnsns.2008.04.002.

4. Ashmawy E.A., Unsteady Couette flow of a micropolar fluid with slip, *Meccanica*, **47**(1): 85–94, 2012, https://doi.org/10.1007/s11012-010-9416-7.

5. Devakar M., Sreenivasu D., Shankar B., Analytical solutions of couple stress fluid flows with slip boundary conditions, *Alexandria Engineering Journal*, **53**(3): 723–730, 2014, https://doi.org/10.1016/j.aej.2014.06.005.

6. Chang Y.C., Keh H.J., Creeping-flow rotation of a slip spherical about its axis of revolution, *Theoretical and Computational Fluid Dynamics*, **26**(1): 173–183, 2012, https://doi.org/10.1007/s00162-010-0216-4.

7. Ashmawy E.A., Slip at the surface of a general axi-symmetric body rotating in a viscous fluid, *Archives of Mechanics*, **63**(4): 341–361, 2011.

8. Prasad M.K., Kaur M., Srinivasacharya D., Slow steady rotation of an approximate sphere in an approximate spherical container with slip surfaces, *International Journal of Applied and Computational Mathematics*, **3**(2): 987–999, 2017, https://doi.org/10.1007/s40819-016-0151-1.

9. Nishad S., Madasu K.P., Effect of spin slip conditions on Couette-Poiseuille flow of couple stress fluid between parallel plates, *Applied and Computational Mechanics*, **18**(2): 175–188, 2024, https://doi.org/ 10.24132/acm.2024.912.

10. Iyenger T.K.V., Srinivasacharya D., Slow steady rotation of an approximate sphere in an in compressible micropolar fluid, *International Journal of Engineering Science*, **33**(6): 867–877, 1995, https://doi.org/10.1016/0020-7225(94)00091-W.

11. El-Sapa S., Saad E.I., Faltas M.S., Axisymmetric motion of two rigid spheres in a Brinkman medium with slip surfaces, *European Journal of Mechanics – B/Fluids*, **67**: 306–313, 2018, https://doi.org/10.1016/j.euromechflu.2017.10.003.

12. Ashmawy E.A., Hydrodynamic interaction between two rotating spheres in an incompressible couple stress fluid, *European Journal of Mechanics – B/Fluids*, **72**: 364–373, 2018, https://doi.org/10.1016/j.euromechflu.2018.07.005.

13. Chou C.Y., Keh H.J., Slow rotation of a spherical particle in an eccentric spherical cavity with slip surfaces, *European Journal of Mechanics – B/Fluids*, **86**: 150–156, 2021, https://doi.org/10.1016/j.euromechflu.2020.12.007.

14. Ashmawy E.A., Unsteady Stokes flow of a couple stress fluid around a rotating sphere with slip, *The European Physical Journal Plus*, **131**(5): 175, 2016, https://doi.org/10.1140/epjp/i2016-16175-6.

15. Al-Hanaya A., El-Sapa S., Ashmawy E.A., Axisymmetric motion of an incompressible couple stress fluid between two eccentric rotating spheres, *Journal of Applied Mechanics and Technical Physics*, **63**(5): 790–798, 2022, https://doi.org/10.1134/S0021894422050078.

16. El-Sapa S., Almoneef A.A., The axisymmetric migration of an aerosol particle embedded in a Brinkmann medium of a couple stress fluid with slip regime, *European Journal of Pure and Applied Mathematics*, **15**(4): 1566–1592, 2022, https://doi.org/10.29020/nybg.ejpam.v15i4.4549.

17. El-Sapa S., Al-Hanaya A., Effects of slippage and permeability of couple stress fluid squeezed between two concentric rotating spheres, *Physics of Fluids*, **35**(10): 103112, 2023, https://doi.org/10.1063/5.0171851.

18. Al-Hanaya A., El-Sapa S., Impact of slippage on the wall correction rotation factor of MHD couple stress fluid between two concentric spheres, *Results in Engineering*, **20**: 101463, 2023, https://doi.org/10.1016/j.rineng.2023.101463.

19. Sarkar P., Madasu K.P., Slow flow of couple stress fluid past a cylinder embedded in a porous medium: slip effect, *Engineering Transactions*, **71**(4): 537–551, 2023, https://doi.org/10.24423/EngTrans.2707.20231010.

20. Alotaibi M.A., El- Sapa S., MHD couple stress fluid between two concentric spheres with slip regime, *Results in Engineering*, **21**: 101934, 2024, https://doi.org/10.1016/j.rineng.2024.101934.

21. Hadjesfandiari A.R., Dargush G.F., Hadjesfandiari A., Consistent skew-symmetric couple stress theory for size-dependent creeping flow, *Journal of Non-Newtonian Fluid Mechanics*, **196**: 83–94, 2013, https://doi.org/10.1016/j.jnnfm.2012.12.012.

22. Happel J., Brenner H., *Low Reynolds Number Hydrodynamics: with Special Applications to Particulate Media*, *Mechanics of Fluids and Transport Processes*, Vol. 1, E-book, Springer Science & Business Media, 2012.

23. Olver F.W.J., Lozier D.W., Boisvert R.F., Clark C.W. [Eds.], *NIST Handbook of Mathematical Functions, Hardback and CD-ROM*, Cambridge University Press, New York, NY, 2010.

24. Arfken G.B., Weber H.J., Harris F.E., *Mathematical Methods for Physicists*, Academic Press, 2012, https://doi.org/10.1016/C2009-0-30629-7.

25. Deo S., Gupta B.R., Stokes flow past a swarm of porous approximately spheroidal particles with Kuwabara boundary condition, *Acta Mechanica*, **203**(3): 241–254, 2009, https://doi.org/10.1007/s00707-008-0048-0.

26. Gupta B.R., Deo S., Axisymmetric creeping flow of a micropolar fluid over a sphere coated with a thin fluid film, *Journal of Applied Fluid Mechanics*, **6**(2): 149–155, 2013, https://doi.org/10.36884/jafm.6.02.19509.

Received August 20, 2024; accepted version February 20, 2025.
Online first May 13, 2025.